PHYSICAL REVIEW B VOLUME 49, NUMBER 7 15 FEBRUARY 1994-I

Multiphonon response in corrugated two-dimensional systems

Hyangsuk Seong and S. D. Mahanti
Department of Physics and Astronomy and the Center for Fundamental Materials Research, Michigan State University, East Lansing, Michigan 48824

(Received 27 October 1993)

The vibrational density of states associated with the in-plane dynamics of intercalants in graphite intercalation compounds obtained from inelastic-neutron-scattering (INS) measurements shows a characteristic two-peak structure. Using molecular-dynamics simulations of screened Coulomb systems on a strongly corrugated substrate we show that the high-frequency peak is due to two-phonon response, thus providing a correct understanding of the INS experiments. The temperature and q dependence of the incoherent dynamic structure factor confirms our picture.

Intercalants inside host layers and atomic overlayers on substrates exhibit a rich variety of structures depending on the size of the intercalants (or atoms), planar density, and the strength and period of the host (or substrate) corrugation potential.[1,2] In particular, melting and dynamic properties of systems that show an incommensurate ground-state structure have been of considerable experimental and theoretical interest.[3,4] For melting, one is interested in the physics underlying domain and domain-wall melting,[1,3,5] and in the existence (in certain systems) of the fluid phase even at zero temperature.[3] As regards dynamics, a fundamental question is how the in-plane vibrational modes reflect and probe the discommensuration structure and intercalant-intercalant and intercalant-substrate interactions.[6–8] Here we address this question, using alkali-metal intercalants inside graphite layers as our model system, and the versatility of molecular dynamics (MD) simulations.

Stage-n graphite intercalation compounds (GIC's) are characterized by a stacking sequence of n graphene layers and an intercalant layer. The most extensive neutron-scattering experiments to probe intercalant dynamics were carried out by Kamitakahara and Zabel (KZ) in alkali-metal GIC's.[7,8] KZ proposed an *unscreened* Coulomb interaction model for the alkali-metal intercalants to explain the observed double-peak structure in the in-plane vibrational density of states $g(\nu)$ they obtained from the experimental dynamic structure factor $S(q,\nu)$.[9] This *unscreened* Coulomb interaction picture is in conflict with the *screened* Coulomb[10] model proposed for these systems, and found to be successful for RbC_{24} in explaining the static structure factor (both in the liquid[11–15] and the solid phases[16]), the solid-liquid phase transition of the intercalants,[12,13] and the low-frequency dynamics in the liquid phase.[14,15]

KZ extracted the phonon density of states (PDOS) $g(\nu)$ from $S(q,\nu)$ using the relation $g(\nu) \propto [n(\nu)+1]S(q,\nu)/\nu$, where $n(\nu)$ is the usual Bose distribution function. [Generally, $g(\nu)$ depends on q.] This is exact for a harmonic solid when $S(q,\nu)$ is the *self-dynamic* structure factor, and if the multiphonon contributions to $S(q,\nu)$ are negligible.[17,18] The two observed peaks in $g(\nu)$ for stage-2 alkali-metal GIC's were assigned to transverse (TA) and longitudinal (LA) acoustic modes. Further, the low-frequency peak (TA) was unusually sharp for an incommensurate system, and was still dominant above the melting temperature, whereas the high-frequency peak (LA) broadened remarkably. This is difficult to understand even when one considers the effect of corrugation; the TA mode should be weaker than the LA mode in the liquid phase.

Although KZ did not carry out lattice-dynamics studies for stage-2 compounds, they could fit $g(\nu)$ obtained from lattice-dynamics calculations to their experiments in stage-1 Rb and K GIC's (where a two-peak structure was also observed) (Refs. 7 and 8) only when they assumed an *unscreened* Coulomb interaction between the intercalants. They assigned the high-frequency peak to the collective mode (plasma oscillation) of unscreened Rb^+ and K^+ ions modified by the corrugation potential. If there is no screening in stage-1 GIC's, there should be also no screening for higher stage GIC's because of their lower electronic density. Therefore one should be able to fit the high-frequency peak in RbC_{24} (KC_{24}) using the *unscreened* Coulomb model. For RbC_{24} (KC_{24}) we find this collective mode frequency to be 1.35 (2.03) THz, which increases to about 1.68 (2.52) THz in the presence of corrugation potential.[19] However, the observed high-frequency peak is 2–2.6 (3–3.5) THz, thus making the *unscreened* Coulomb model unsatisfactory.

To understand these puzzling issues, we have calculated the PDOS using MD simulation. Although KZ made extensive studies for many alkali-metal GIC's, we will focus on RbC_{24} because of successful studies in this system with the repulsive *screened* Coulomb potential model.[11–14] A distinct advantage of MD simulations is that one can obtain easily the self-part of $S(q,\nu)$, i.e., $S_{\text{incoh}}(q,\nu)$, and by probing this quantity at different length scales one can separate single-phonon and multiphonon processes, something impossible to do in experiments when the intercalants are coherent scatterers such as alkali-metal atoms. We argue that the previous interpretation of the two-peak structure seen in inelastic-neutron-scattering (INS) experiments at large q (Refs. 7 and 8) is incorrect, and we provide a correct explanation of the INS spectrum in terms of a multiphonon response whose pronounced spectral weight is a consequence of the strong corrugation. In fact, this multiphonon peak is seen even in the liquid phase, a characteristic feature of a lattice fluid.

For RbC_{24}, whose ground state is an incommensurate structure,[16,20] it is not simple to calculate the harmonic PDOS

$$g_H(\nu)=\frac{1}{2N}\sum_{i=1}^{2N}\delta(\nu-\nu_i) \tag{1}$$

associated with the dynamics of Rb ions via the usual lattice-dynamics calculations; ν_i's in Eq. (1) are the frequencies of $2N$ planar modes. Vibrations of intercalants perpendicular to the graphite layers are not considered here. One way to handle this problem is through MD simulations. The Fourier transform of the velocity autocorrelation function (VAF) for a harmonic system is directly related to $g_H(\nu)$.[21] In this paper, we study the PDOS obtained via both the Fourier transform of VAF [denoted as $g_H(\nu)$] and the incoherent dynamic structure factor [denoted as $g(\nu)$] using MD simulation. Our results for $g(\nu)$ not only agree with that obtained from the INS experiments,[7] but also elucidate both the origin of the two-peak structure and the nature of interaction between the alkali-metal intercalants. The relationship between $g(\nu)$ and the harmonic density of states $g_H(\nu)$ becomes transparent by looking at the temperature (T) and q dependence of $g(\nu)$. The details of the MD simulations can be found in our earlier publications.[13,16]

To understand the experimental results, we review the procedure KZ used to obtain $g(\nu)$ from neutron-scattering data. Although Rb is a coherent scatterer, for sufficiently *large* q and for all possible planar orientations, one can use the incoherent approximation,[22] i.e., $S(q,\nu)\simeq S_{\rm incoh}(q,\nu)$. For a harmonic solid, $S_{\rm incoh}(q,\nu)$ can be expanded as follows:[18]

$$\begin{aligned}S_{\rm incoh}(q,\nu)&=\sum_p S^p_{\rm incoh}(q,\nu)\\&=\sum_p e^{-2W(q)}\frac{1}{p!}\left[\frac{hq^2}{4\pi m}\right]^p\\&\quad\times\prod_{i=1}^{p}\left[\int_{-\infty}^{\infty}d\nu_i\frac{g_H(\nu_i)}{2\pi\nu_i}n(\nu_i)\right]\\&\quad\times\delta\left[\nu+\sum_{i=1}^{p}\nu_i\right],\end{aligned} \tag{2}$$

where p corresponds to the p-phonon contribution, and $W(q)$ is the Debye-Waller factor. The one- and two-phonon contributions in Eq. (2) are

$$S^1_{\rm incoh}(q,\nu)=e^{-2W(q)}\frac{hq^2}{8\pi^2 m}\frac{n(\nu)+1}{\nu}g_H(\nu)\ , \tag{3}$$

$$\begin{aligned}S^2_{\rm incoh}(q,\nu)&=e^{-2W(q)}\frac{1}{2!}\left[\frac{hq^2}{8\pi^2 m}\right]^2\\&\quad\times\int_{-\infty}^{\infty}d\nu_1\frac{g_H(\nu_1)g_H(-\nu-\nu_1)}{\nu_1(-\nu-\nu_1)}\\&\quad\times n(\nu_1)n(-\nu-\nu_1)\ .\end{aligned} \tag{4}$$

We define a new function $A(q,\nu)$ given by

$$A(q,\nu)=S_{\rm incoh}(q,\nu)\frac{\nu}{n(\nu)+1}\ . \tag{5}$$

This $A(q,\nu)$ is what KZ referred to as $g(\nu)$ (Ref. 23) within a normalization constant which depends on q and T. If the one-phonon term in Eq. (2) is dominant, then one can obtain $g_H(\nu)$ from $S_{\rm incoh}(q,\nu)$, i.e.,

$$A(q,\nu)\simeq S^1_{\rm incoh}(q,\nu)\frac{\nu}{n(\nu)+1}\sim g_H(\nu)\ . \tag{6}$$

Therefore, when (1) the incoherent approximation is valid, and (2) multiple-phonon contributions to $S_{\rm incoh}(q,\nu)$ are negligible, $A(q,\nu)$ is the PDOS associated with one-phonon excitations. Thus $g(\nu)$ is equal to $g_H(\nu)$ only when the two above approximations are valid, and in general they should not be equal.

Let us now calculate $S(q,\nu)$ and $A(q,\nu)$ using MD simulations at $q=4$ Å^{-1}, which is in the range of the q values used by KZ. Figure 1 (upper panel) gives the experimental $S(q,\nu)$ at 210 K,[7] and our calculated $S(q,\nu)$ for the liquid at 248 K. The reason we have chosen a slightly higher temperature to compare the experimental data is because the melting temperature with our potential is 220 K,[13] compared to an experimental value of 165 K.[12] Clearly the agreement is remarkable. In the lower panel we give the calculated $A(q=4,\nu)$ for two different

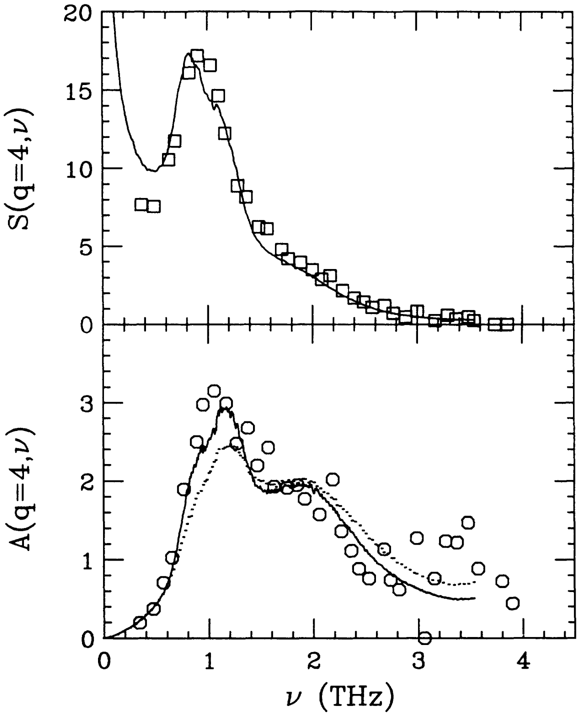

FIG. 1. The symbols are experimental data, and the solid lines are MD simulations for RbC_{24} in the liquid phase. MD results have been scaled to fit the experimental data which are in arbitrary units. Upper panel: $S(q,\nu)$ at $q=4$ Å^{-1}. Lower panel: $g(\nu)=A(q=4,\nu)$ obtained from the MD simulation at 248 (solid line) and 299 K (dotted line), and compared with experimental $g(q,\nu)$. The experimental resolution is ~0.3 THz near 1 THz, and ~1 THz near 3 THz.

temperatures. Again the agreement between MD at 248 K and experimental $g(\nu)$ is good. The discrepancy seen in $A(q,\nu)$ is due to (1) multiphonon corrections made by KZ to $S(q,\nu)$, and (2) any additional scattering in the high-frequency region (3–4 THz) which is accentuated in going from $S(q,\nu)$ to $g(\nu)$ due to the multiplication factor $\nu/[n(\nu)+1]$. To understand the origin of the high-frequency peak in $g(\nu)$ at 2 THz, we increase the temperature to 299 K and see an increase in the relative weight in the high-frequency peak compared to that in the low frequency. When we increase T to about twice the melting temperature, the intensities of the two peaks become comparable. This is clearly seen in the experiments for both KC_{24} and RbC_{24},[7,8] thus confirming the two-phonon origin of the high-frequency peak seen in $g(\nu)$.

The large intensity seen in the experiment near 3–4 THz (where the experimental resolution is about 1 THz) is most likely due to the intercalant dynamics perpendicular to the graphite plane, because dispersion curves for the $(00q)$LA modes show frequencies up to 4 THz.[8] Since polarizations of phonon modes are well defined in the solid, these perpendicular modes should show up in $g(\nu)$ more prominently in the solid phase due to the mosaicity of the samples. In Fig. 2, we give the results for the solid at 144 K which indeed show a large discrepancy in the high-frequency region. The doublet structure we obtain near 1 THz is from the TA and LA modes; it is not seen in the experiment since the energy resolution is ~0.3 THz.[7] When we cool the solid to 125 K, we find the relative intensity of the high-frequency peak decreases, which further supports the multiphonon explanation.

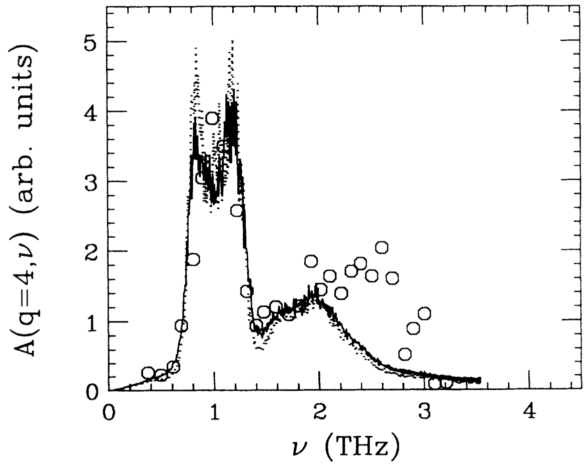

FIG. 2. Temperature dependence of the two-phonon contribution (using MD) to $A(q,\nu)$ at $q=4$ Å^{-1} for RbC_{24} at two different temperatures $T=144$ [$\sim 0.6T_m$, where the melting temperature $T_m=220$ K (Ref. 13)] (solid line) and 125 K (dotted line). Experimental data (circles) are in the solid state at 100 K ($\sim 0.6T_m$, where experimental $T_m \sim 165$ K). The discrepancy in the high-frequency region is likely due to the intercalant modes perpendicular to the layer.

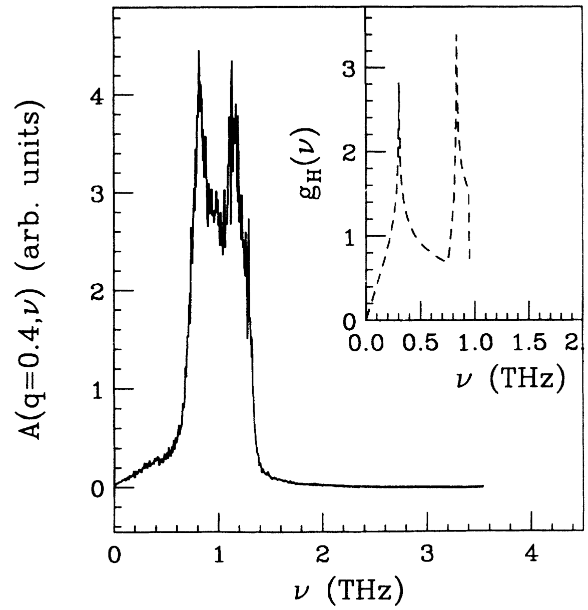

FIG. 3. $A(q,\nu)$ at $q=0.4$ Å^{-1}. This is found to be a replica of the Fourier transform of VAF, $g_H(\nu)$. The inset gives $g_H(\nu)$ for the same system in the absence of corrugation potential.

In addition to the temperature dependence, the p-phonon contribution to $S_{\text{incoh}}(q,\nu)$ [and therefore to $g(\nu)$] is proportional to the q^{2p} [see Eq. (2)]. The characteristic dimensionless quantity that determines this q dependence is the ratio ν_q/ν_H, where $\nu_q = hq^2/8\pi^2 m$, ν_H is the harmonic phonon frequency, and m is the mass of the oscillator. Therefore multiphonon processes should be suppressed at *small* q.[17] Since we are not restricted only to large values of q to pick up the incoherent part of the dynamic structure factor, we calculated $A(q,\nu)$ for $q=0.4$ Å^{-1} (Fig. 3), which does not show any high-frequency peak and is found to be a replica of the Fourier transform of the VAF. Thus, to obtain the correct one-

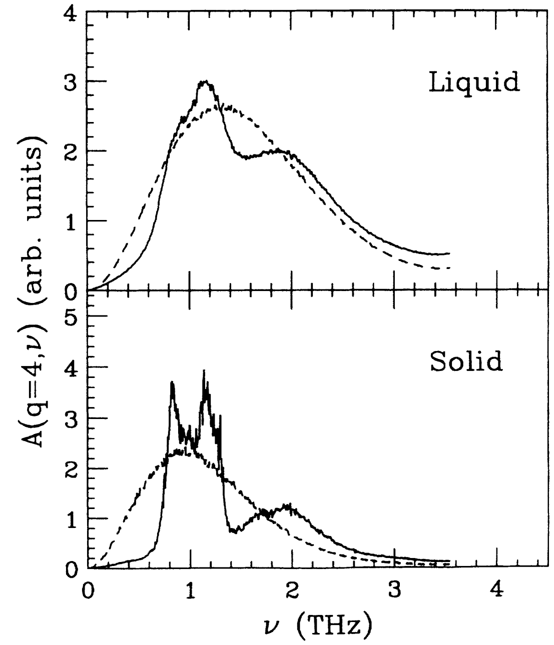

FIG. 4. $A(q,\nu)$ at $q=4$ Å^{-1}. The solid lines are for the RbC_{24}, and the dashed lines are for the system without corrugation potential. The top and bottom panels correspond to the liquid and solid, respectively.

phonon density of states $g_H(\nu)$ via $S_{\mathrm{incoh}}(q,\nu)$, one must confine oneself to small values of q for which Eq. (6) is valid.[17] However, this is difficult experimentally since Rb ions are strong coherent scatterers, and, for small q, coherent scattering dominates in the INS spectrum. From the result of $A(q=0.4,\nu)$, we assign the LA-mode frequency peak to 1.2 THz. When we compare this with the bare plasma frequency $\nu_p=1.35$ THz, we find that the screening effect in stage-2 alkali-metal GIC's is not as large as pure alkali metals, which show a 0.2–0.5 reduction of the bare plasma frequency.

Stage-1 alkali-metal GIC's also show a similar two-peak structure in $g(\nu)$ in the solid phase (see Fig. 4.27 of Ref. 8). We have not made an extensive MD study of these systems because of the unavailability of good interparticle potential. However, making a simple single harmonic-oscillator model with ν_H equal to the lower-peak frequency, we estimate that the weight in the high-frequency peak at $2\nu_H$ is about 60–80 % of that at ν_H at 300 K, qualitatively consistent with experiment.[8]

Finally, to single out the effect of corrugation on both one and multiple PDOS, we calculate $g_H(\nu)$ for a repulsive screened Coulomb system with the same density as RbC_{24} but in the *absence* of the graphite corrugation potential (see inset in Fig. 3). We find that $g_H(\nu)$ is broad and has appreciable value at low frequencies. Thus the corrugation potential strongly suppresses the low-frequency modes in RbC_{24}. One important feature of $A(q=0.4,\nu)$ in RbC_{24} is its narrow width (~ 0.5 THz), which not only gives the sharp low-frequency peak near 1 THz seen in experimental $g(\nu)$, but also leads to a pronounced well-defined two-phonon peak when q is large. For the corrugation free case, $g_H(\nu)$ is large at low frequencies, and consequently $A(q=4,\nu)$ in Fig. 4 does not show any discernible multiphonon peak in either the liquid or the solid phases. Thus a strong corrugation potential is necessary for one to observe multiphonon peaks in $g(\nu)$ or $A(q,\nu)$ at large q. In fact, it should be a characteristic feature of many two-dimensional (2D) systems in the presence of strong corrugation.

In conclusion, we have addressed the in-plane intercalant dynamics of a 2D-corrugated system using MD simulations which give both the $S_{\mathrm{incoh}}(q,\nu)$ and the Fourier transform of the VAF. From the T and q dependences of $A(q,\nu)$ [see Eq. (6)], we obtain a clear understanding of the origin of the two peaks in the PDOS obtained from the INS experiments in alkali-metal GIC's. The INS experiments of Kamitakahara and Zabel[7] for RbC_{24} have been reproduced by MD simulations using a *screened* Coulomb model, indicating that this model not only explains the structure,[16] thermodynamics,[13] and low-frequency liquid dynamics[15] of this system but also its high-frequency ion dynamics as well, thus clarifying the puzzling situation discussed in the beginning of this paper. Finally, the general ideas discussed in this paper are directly relevant to INS experiments in other alkali-metal GIC's and systems such as alkali-metal atoms, H_2, and HD overlayers on different substrates.

We thank Dr. Tahir Çağin for making available to us the MD code. We also thank Professor H. Zabel and Professor S. Moss for helpful discussions. This work was supported by the Center for Fundamental Materials Research and NSF DMR Grant Nos. 89-03579 and 90-24955.

---

[1] R. J. Birgeneau and P. M. Horn, Science **232**, 329 (1986); F. F. Abraham, Adv. Phys. **35**, 1 (1986).

[2] *Graphite Intercalation Compounds, Vol. 1; Structure and Dynamics*, edited by H. Zabel and S. A. Solin, Springer Series on Topics in Current Physics (Springer, New York, 1990).

[3] S. N. Coppersmith *et al.*, Phys. Rev. B **25**, 349 (1982).

[4] Edward Vives and Per-Anker Lindgard (unpublished).

[5] W. A. Steele (unpublished).

[6] M. Nielson, J. P. McTague, and L. Passell (unpublished).

[7] W. A. Kamitakahara and H. Zabel, Phys. Rev. B **32**, 7817 (1985).

[8] H. Zabel, in Ref. 2, p. 101.

[9] KZ justified the use of unscreened Coulomb model by referring to the work of DiVincenzo and Mele [Phys. Rev. B **32**, 2538 (1985)], who, however, treated the problem of screening of a single impurity in graphite, which is not relevant to the screening in GIC's where additional electrons are present in the conduction band.

[10] M. Plischke, Can. J. Phys. **59**, 802 (1981); M. Plischke and W. D. Leckie, *ibid.* **60**, 1139 (1982); P. B. Visscher and L. M. Falicov, Phys. Rev. B **3**, 2541 (1971).

[11] Zhuo-Min Chen, Omar A. Karim, and B. Montgomery Pettitt, J. Chem. Phys. **89**, 1042 (1988).

[12] S. C. Moss and R. Moret, in Ref. 2, p. 5.

[13] Hyangsuk Seong, S. D. Mahanti, Surajit Sen, and Tahir Çağin, Phys. Rev. B **46**, 8748 (1992).

[14] J. D. Fan, George Reiter, and S. C. Moss, Phys. Rev. Lett. **64**, 188 (1990).

[15] Hyangsuk Seong and S. D. Mahanti (unpublished).

[16] Hyangsuk Seong, Surajit Sen, Tahir Çağin, and S. D. Mahanti, Phys. Rev. B **45**, 8841 (1992).

[17] P. A. Egelstaff, in *Dynamics of Disordered Materials*, edited by D. Richter, A. J. Dianoux, W. Petry, and J. Teixeira (unpublished).

[18] W. Marshall and S. W. Lovesey, *Theory of Thermal Neutron Scattering* (Oxford University Press, Oxford, 1971).

[19] We calculated $\nu_c=\sqrt{\nu_0^2+\nu_p^2}$ where ν_0 is the pinning frequency due to the corrugation potential (Ref. 8). The value of ν_0 we obtain from the Fig. 4.28 in Ref. 8 is 1.5 THz (1 THz) for KC_{24} (RbC_{24}) which is an overestimate. Actually, we get $\nu_0 \sim 0.7$ THz for RbC_{24} from Fig. 3 of this paper.

[20] R. Clarke, J. N. Gray, H. Homma, and M. J. Winokur, Phys. Rev. Lett. **47**, 1407 (1981); H. Zabel *et al.*, *ibid.* **57**, 2041 (1986).

[21] A. Rahman, M. J. Mandel, and J. P. McTague, J. Chem. Phys. **64**, 1564 (1976).

[22] M. M. Bredov *et al.*, Fiz. Tverd. Tela (Leningrad) **9**, 287 (1967) [Sov. Phys. Solid State **9**, 214 (1967)].

[23] Although KZ applied some corrections (to estimate multiphonon and other background effects), these corrections are found to be small, and both the corrected and uncorrected data show the same characteristics [Hyangsuk Seong and S.D. Mahanti (unpublished)], namely a prominent peak near 1 THz and a weak peak near 2 THz (for liquid RbC_{24}).